Nuclear Physics B334 (1990) 581–610
North-Holland

ASYMPTOTIC FREEDOM AND MASS GENERATION IN THE O(3) NONLINEAR σ-MODEL

Ulli WOLFF

Institut für Theoretische Physik, Universität Kiel, D-2300 Kiel, FRG

Received 23 February 1989
(Revised 21 August 1989)

We complement a recently discovered collective Monte Carlo algorithm with a cluster variance reduction technique for the two-point function of σ-models. It is used to determine both the nonperturbative mass and the asymptotic freedom scale $\Lambda_{\overline{\rm MS}}$ from simulations of the O(3)-model with correlation lengths up to 121 on large lattices. We also estimate $\Lambda_{\overline{\rm MS}}$ in lattice units by studying the mass gap in physically small volumes. Asymptotic scaling with the bare coupling still does not occur. We propose an approximate lattice β-function that goes beyond finite-order perturbation theory and leads to better scaling behavior. The various methods give $m/\Lambda_{\overline{\rm MS}} = 2.5$–$3.0$ for the O(3)-model.

1. Introduction

In two dimensions the globally O(n) invariant nonlinear σ-models share the property of asymptotic freedom with four-dimensional gauge theories if the symmetry group is nonabelian ($n \geq 3$) [1]. As a consequence one hopes that the short distance physics can be reliably controlled by renormalized perturbation theory which looks structurally similar in the two cases, although it is complicated by gauge invariance. Most of the celebrated phenomenological successes of QCD to date are based on this assumption. At large distance either theory is expected to nonperturbatively generate a physical scale, namely the mass gap in the σ-model and the string tension between static quarks in QCD. At present, the nonperturbative physics can only directly be accessed by numerical simulations in a formulation employing a lattice cutoff. We are then dealing with classical statistical systems in two or four euclidean dimensions and apply Monte Carlo techniques to them. It is highly nontrivial to convince oneself that in this way one really computes universal features of the same theory that is partially evaluated in perturbation theory by rather different techniques (e.g. dimensional regularization). The notorious difficulties to verify the presence or absence of scaling are closely related to this kind of questions of consistency. The main problem is that the nonperturbative scale corresponds to the correlation length ξ of the statistical system. As such it has to

satisfy several physical constraints in a realistic field theoretic simulation: The overall extension of the system has to be several ξ in all directions to avoid strong finite-size effects. At the same time ξ has to be large compared to the lattice spacing ($=1$ in lattice units) to separate the ultraviolet cutoff scale from physical scales. The perturbative regime is now expected to lie at lattice distances x which fulfill $1 \ll |x| \ll \xi$. Unfortunately, it has been very hard so far to perform simulations at large enough correlation length to satisfy all the above constraints and leave enough room to probe perturbative and nonperturbative physics in the same Monte Carlo run.

The main reason for this dilemma, at least in the two-dimensional spin models, was the phenomenon of critical slowing down: Once the correlation length exceeds a few lattice spacings, it takes an excessive number of iterations with standard algorithms to generate independent unbiased estimates of physical quantities. Elaborating on the Swendsen–Wang algorithm for Potts models [2], a new kind of collective Monte Carlo algorithm has recently been developed [3] and shown to eliminate slowing down in the x–y model [4] in the following sense: As we simultaneously scaled up correlation length and sample size, the autocorrelation time in CPU units (operations per spin) remained constant. The algorithm also performs favorably in the nonabelian case. We use it in the present study to determine the ratio of the mass gap to the perturbatively introduced Λ-parameter solely from the correlation at appropriate separations in the scaling regime of the theory. This is achieved by high precision simulations with ξ up to 121 in the O(3)-model.

Another possibility to relate the lattice scale to the perturbative scale has been pointed out by Lüscher [5]. The mass gap in a physically small volume with extension of order ξ or less can be computed in perturbation theory. If it is determined in a simulation at a bare coupling where one also knows the large volume mass gap, and if the perturbative calculation is sufficiently accurate, then the desired ratio of short-to-long distance scales follows, too. With standard algorithms such a calculation suffers from similar problems as discussed before. It has been attempted in ref. [6]. Due to the algorithmic limitations the evidence for scaling and universality in the O(3)-model has not been overwhelming, and the numerical estimates for the mass in Λ-units scatter by a factor of about three in the literature. (Some earlier simulations of the O(3) model are given in ref. [7].)

We also report on a further algorithmic improvement in connection with the new algorithm in the form of variance reduction or improved estimators. It boosts the efficiency of the simulation in the interesting parameter range by at least another order of magnitude.

The paper is organized as follows: In sect. 2 the variance reduction technique is presented. In sect. 3 we analyze the correction function by fitting it to its theoretical scaling forms at large and small distances. In sect. 4 data on the mass gap for physically small volumes are reported and discussed. The issue of scaling with the

bare lattice coupling is discussed in sect. 5, and conclusions follow in sect. 6. In appendices A and B the universal short distance behavior of the two-point function is derived by continuum perturbation theory and by using the renormalization group.

2. Improved estimators and collective algorithms

In this section we shall demonstrate that the percolation clusters appearing in the collective updating process can further be used to define improved estimators for physical observables. They are quantities that are rigorously shown to have the same mean as some correlation functions with a variance that is smaller than the one of the naive expression in terms of elementary fields. To bring out the general idea we consider an abstract observable $\mathcal{O}(\sigma)$ averaged over field configurations σ with some action $S(\sigma)$,

$$\langle \mathcal{O} \rangle = \frac{1}{Z} \int \mathrm{D}\sigma \, \mathrm{e}^{-S(\sigma)} \mathcal{O}(\sigma), \tag{2.1}$$

where the normalization factor Z is the partition function. Any set of transition probabilities $W(\sigma \to \sigma')$ that lead to a valid Monte Carlo process for (2.1) obey

$$\int \mathrm{D}\sigma \, \mathrm{e}^{-S(\sigma)} W(\sigma \to \sigma') = \mathrm{e}^{-S(\sigma')}, \tag{2.2}$$

i.e. they leave the Boltzmann distribution invariant. Apart from updating we may also employ W to define an observable

$$\tilde{\mathcal{O}}(\sigma) = \int \mathrm{D}\sigma' \, W(\sigma \to \sigma') \mathcal{O}(\sigma'), \tag{2.3}$$

and $\tilde{\mathcal{O}}$ and $\mathcal{O}$ trivially have the same mean due to eq. (2.2). Relation (2.3) can become powerful if the summation over σ' can at least partly be carried out exactly. Then, for each σ that is sampled, the whole class of σ' that is summed over contributes to the expectation value. Note that W in eq. (2.3) does not have to be identical with the probabilities used for updating, and, if different, it does not necessarily have to be ergodic for the present purpose. The well-known variance reduction technique [8], for example, is obtained by using the heatbath form for W with local changes of fields just at the lattice sites where correlations are to be evaluated. Thus the observable is "delocalized" by one or a few lattice spacings, and one is rewarded by the reduced variance for collecting more information in the measurement. In ref. [9] it was found that a truly nonlocal transformation can lead to very significant gains, and this will be exploited now in connection with the new collective algorithm [3, 4].

From here on we specialize the discussion to the O(n) σ-models,

$$Z = \prod_x \int_{S_{n-1}} d\sigma_x \exp\Big(\beta \sum_{x\mu} \sigma_x \cdot \sigma_{x+\mu} \Big), \tag{2.4}$$

with the same notation as in ref. [4]. For nonlocal updating we choose a random direction $r \in S_{n-1}$ and activate links $\langle xy \rangle$ with probability

$$p_r(\sigma_x, \sigma_y) = 1 - \exp\big\{ \min\big[0, -2\beta \sigma_x \cdot r \sigma_y \cdot r\big] \big\}. \tag{2.5}$$

The resulting auxiliary bond percolation problem now defines a decomposition of the $|\Lambda| = L^2$ sites of the periodic square lattice Λ into N_c disconnected components or clusters

$$\Lambda = \bigcup_{i=1}^{i=N_c} c_i . \tag{2.6}$$

A class of algorithms including the one described in refs. [3,4] is constructed by next choosing one cluster $C \subseteq \Lambda$, which is a union of some of the components in $\{c_i\}$ by some probabilistic process governed by probabilities $M(\{c_i\}, C)$. We then flip the r-component of spins on C and have an overall transition probability to a new configuration σ' given by

$$W(\sigma \to \sigma') = \int dr \sum_{\{c_i\}} K_r(\sigma, \{c_i\}) \sum_C M(\{c_i\}, C) \delta(\sigma', R^C \sigma). \tag{2.7}$$

In eq. (2.7) K_r is the probability to build a certain cluster structure $\{c_i\}$, and the first sum is over all possible decompositions. The second sum is over single clusters, and the δ-function and flip operation R^C on C,

$$(R^C \sigma)_x = \begin{cases} \sigma_x - 2(\sigma_x \cdot r) r & \text{if } \sigma_x \in C, \\ \sigma_x & \text{if } \sigma_x \notin C, \end{cases} \tag{2.8}$$

have been defined in ref. [4]. The algorithm in refs. [3,4] amounts to choosing one of the components c_i with probability proportional to their sizes,

$$M_1(\{c_i\}, C) = \sum_{i=1}^{N_c} \frac{|c_i|}{|\Lambda|} \delta_{c_i, C}, \tag{2.9}$$

and we shall refer to it as the one cluster (1C) method. A generalization (to continuous many component spins) of the Swendsen–Wang (SW) algorithm [2] is

given by $M_{\mathrm{SW}}(\{c_i\},C)$, which is obtained by including in C each component c_i independently with probability 1/2.

For M_1 we proved detailed balance in ref. [4]. Here we shall also need M_{SW}, and, in fact, detailed balance will now be demonstrated for arbitrary M. As discussed in ref. [4], a transition between given σ and $\sigma' = R^C\sigma$ can proceed only through unique C and $\pm r$ apart from a set of configurations of measure zero. Therefore

$$\frac{W(\sigma\to\sigma')}{W(\sigma'\to\sigma)} = \frac{\Sigma_{\{c_i\}} K_r(\sigma,\{c_i\}) M(\{c_i\},C)}{\Sigma_{\{c_i\}} K_r(\sigma',\{c_i\}) M(\{c_i\},C)} \tag{2.10}$$

holds. Also, C defines a unique set of surface bonds ∂C, and in the percolation processes leading to any of the $\{c_i\}$ contributing in (2.10) these surface bonds cannot be activated. Moreover, the activation probabilities for bonds in ∂C are the only ones differing as one starts from σ or from σ'. If we cancel the "nonactivation" probabilities on ∂C, we get the equality

$$\frac{K_r(\sigma,\{c_i\})}{\prod_{\langle xy\rangle\in\partial C}(1-p_r(\sigma_x,\sigma_y))} = \frac{K_r(\sigma',\{c_i\})}{\prod_{\langle xy\rangle\in\partial C}(1-p_r(\sigma'_x,\sigma'_y))} \tag{2.11}$$

for all $\{c_i\}$ contributing in eq. (2.10). If one inserts eq. (2.11) with eq. (2.5) into eq. (2.10), the detailed balance equation follows. One could use the freedom of selecting M to influence the size distribution of flipped clusters if this should become necessary (in more than two dimensions, for example). The 1C method has however the special virtue that one can construct C without analyzing all c_i.

We now consider the observable

$$\mathcal{O}(\sigma) = \sigma_x\cdot\sigma_y, \tag{2.12}$$

corresponding to the two-point function and improve it as in eq. (2.3) using the SW process,

$$\begin{aligned}\tilde{\mathcal{O}}(\sigma) &= \int dr \sum_{\{c_i\}} K_r(\sigma,\{c_i\}) \sum_C M_{\mathrm{SW}}(\{c_i\},C)(R^C\sigma)_x\cdot(R^C\sigma)_y \\ &= \int dr \left(\sigma_x\cdot(1-P_r)\sigma_y + \sum_{\{c_i\}} K_r(\sigma,\{c_i\}) \sum_C M_{\mathrm{SW}}(\{c_i\},C)(R^C\sigma)_x\cdot P_r(R^C\sigma)_y\right).\end{aligned} \tag{2.13}$$

Here we introduced the spin projector in the r-direction, $P_r\sigma_x = r(r\cdot\sigma_x)$, and used the fact that the perpendicular components of all spins remain unchanged. The

average of that part is by O(n) symmetry

$$\left\langle \int \mathrm{d}r\, \sigma_x \cdot (1 - P_r)\sigma_y \right\rangle = (1 - 1/n)\langle \sigma_x \cdot \sigma_y \rangle , \tag{2.14}$$

as one simply drops one of the n components in the scalar product. In the sum over C in eq. (2.13) each of the components c_i belongs to C "half of the time". It is easy to see now that whenever x and y lie in different c_i, the C-sum vanishes as the product of the r-components in $(R^{\mathrm{C}}\sigma)_x$ and $(R^{\mathrm{C}}\sigma)_y$ are as often positive as negative and have constant magnitude. The two-point function is thus also given by $\langle \tilde{\mathcal{O}} \rangle$ with

$$\mathcal{O}(\sigma) = n \int \mathrm{d}r\, K_r(\sigma, \{\mathrm{c}_i\}) \sum_i \Theta(\mathrm{c}_i, x)\Theta(\mathrm{c}_i, y)(r \cdot \sigma_x)(r \cdot \sigma_y) . \tag{2.15}$$

The sum over C has been carried out by the normalization of M_{SW} as a probability, and the characteristic function Θ is defined as

$$\Theta(\mathrm{c}_i, x) = \begin{cases} 1 & \text{if } x \in \mathrm{c}_i , \\ 0 & \text{otherwise} . \end{cases} \tag{2.16}$$

Finally we adapt eq. (2.15) to the 1C-process by introducing M_1,

$$\tilde{\mathcal{O}}(\sigma) = n \int \mathrm{d}r\, K_r(\sigma, \{\mathrm{c}_i\}) \sum_{\mathrm{C}} M_1(\{\mathrm{c}_i\}, \mathrm{C}) \frac{|\Lambda|}{|\mathrm{C}|} \Theta(\mathrm{C}, x)\Theta(\mathrm{C}, y)(r \cdot \sigma_x)(r \cdot \sigma_y) . \tag{2.17}$$

Referring now under the average $\langle \ldots \rangle$ to the clusters C and directions r appearing in the 1C-update process, we may summarize our construction as

$$\langle \sigma_x \cdot \sigma_y \rangle = n \left\langle \frac{|\Lambda|}{|\mathrm{C}|} (r \cdot \sigma_x)(r \cdot \sigma_y) \Theta(\mathrm{C}, x)\Theta(\mathrm{C}, y) \right\rangle . \tag{2.18}$$

Eq. (2.18) constitutes a rather remarkable simplification for estimating the fundamental correlation function in the σ-model. All quantities on the right-hand side are accessible at almost no extra cost in CPU time as they appear in the cluster construction [3]. The cluster probabilities (2.5) imply that $r \cdot \sigma_x$ has only one sign for all $x \in \mathrm{C}$, i.e. our observable is positive. The exponential decay of the correlation is thus produced by the cluster size distribution rather than by sign cancellations, and we shall find a strongly reduced variance for the simple reasons given in ref. [9]. It fits nicely with this picture that we observed that

$$\langle |\mathrm{C}| \rangle = k(n)\, \chi \tag{2.19}$$

gives the average cluster size for O(n)-models in terms of the susceptibility χ anywhere in the scaling region. For $k(n)$ we found $k(1) = 1$ (exact), $k(2) \cong 0.81$ ([4]), and $k(3) \cong 0.75$ (this paper). Consequences of summations over x, y in (2.18) are

$$1/n = \left\langle \frac{1}{|C|} \sum_{x \in C} (r \cdot \sigma_x)^2 \right\rangle \tag{2.20}$$

giving the average r-component of spins aggregating to a cluster, and

$$\chi = \frac{1}{|A|} \left\langle \left(\sum_x \sigma_x \right)^2 \right\rangle = n \left\langle \frac{1}{|C|} \left(\sum_{x \in C} r \cdot \sigma_x \right)^2 \right\rangle \tag{2.21}$$

relating the magnetic susceptibility to an average r-component susceptibility in the flipped cluster.

We conclude this section by forestalling some practical experiences with measuring correlations by eq. (2.18). We simulated the O(3) model on a 128^2 lattice at $\xi \cong 11$ ($\beta = 1.5$). For the same number of cluster update steps we determined the mass gap by fits to zero momentum correlations between separations 10 and 60 with standard estimators and with eq. (2.18). In the latter case the error turns out to be about four times smaller. With the time needed for measuring being small compared to updating, we have thus gained a factor 16 in the CPU time it takes to measure the correlation length to a given accuracy. As the gain grows with separation [9] we are enabled to move to relatively large distances for fitting masses without unreasonably increasing errors. This is highly welcome as, with the improved statistical quality of the new algorithm, we can now also reduce systematic errors in masses, which otherwise could become a new limitation. On the largest lattice in this study (512×800), the errors (from binning) when determining $\xi \cong 121$ from correlations at distances 121 to 400 or from 363 to 400 differ by a factor of less than two. As for autocorrelations we shall find that measuring (2.18) after each cluster in the simulation effectively represents an almost independent estimate. This means that – once we have equilibrated the lattice – we produce an independent low variance estimate for the two-point correlation at all distances with an average CPU-work of O(χ) ($\cong$ correlation volume) operations. This refers to an implementation of the 1C algorithm as presented in ref. [3].

3. Correlation function at long and short distance

The O(n)-invariant spin–spin two-point correlation function can be used in a lattice simulation to derive both the nonperturbative mass gap and the asymptotic freedom scale. We estimate the mass gap m in the O(3)-model by fitting the zero

TABLE 1
Large volume results for the mass gap m and susceptibility χ of the O(3) σ-model. The number of generated clusters is #C, and ε and $\bar{\tau}$ characterize autocorrelations

β	T	L	#C/10^6	m^{-1}	χ	$\bar{\tau}$	$\varepsilon\bar{\tau}$
1.4	64	64	4.1	6.90(1)	78.9(1)	–	–
1.5	128	128	6.1	11.09(2)	176.3(2)	120	0.4
1.6	256	256	2.6	19.07(6)	451.2(8)	100	0.2
1.7	256	256	2.6	34.57(7)	1262(3)	70	0.3
1.8	512	512	2.6	64.78(15)	3832(7)	80	0.3
1.9	800	512	0.64	121.2(6)	11561(48)	40	0.4

spatial momentum correlation function to the form

$$\sum_{\substack{x=(x_1,\,x_2)\\ y=(y_1,\,x_2+t)}} \langle \sigma_x \cdot \sigma_y \rangle = A\left(\mathrm{e}^{-tm} + \mathrm{e}^{-(T-t)m}\right). \tag{3.1}$$

Here the space components (1) of x and y are summed independently over all space of length L to project on zero momentum. The time coordinates (2) are kept at variable separation $0 \leqslant t \leqslant T/2$, and time periodicity T is properly taken into account. For the fit only large enough t-values must be used, where the contributions of states of higher energy than the lowest zero momentum state above the vacuum are negligible. We performed all mass fits by selfconsistently starting the fits at about $t = m^{-1}$, $2m^{-1}$, and $3m^{-1}$ up to $T/2$. The expected systematic trend to smaller m-values is just visible, but it is never larger than our small statistical errors which are determined by the usual binning procedure. We decided to quote all mass values in this paper from fits starting at $2m^{-1}$. Results for a number of β-values are found in the first columns of table 1 together with the lattice size and the number of clusters #C generated, which equals the number of estimates of the two-function.

Also in this study we made an effort to analyze the structure of autocorrelations between the improved estimates related to successive update clusters. We define the autocorrelation function

$$\Gamma(t) = \langle \tilde{\chi}_s \tilde{\chi}_{s+t} \rangle - \langle \tilde{\chi}_s \rangle^2, \tag{3.2}$$

where $\tilde{\chi}_s$ is the improved estimator for the susceptibility (2.21) from the sth cluster in the simulation. We choose χ here as a representative long-range quantity. We found that typically $\Gamma(t)$ drops by a factor of order 100 from $t = 0$ to $t = 1$, and that only for $t \geqslant 1$ it behaves roughly exponentially with a scale $\bar{\tau} \gg 1$. For this reason we try to estimate not only the usual integrated autocorrelation time [10], but separately

$$\varepsilon = \Gamma(1)/\Gamma(0) \tag{3.3}$$

and

$$\bar{\tau} = \frac{1}{\Gamma(1)} \sum_{t=1}^{\infty} \Gamma(t) . \tag{3.4}$$

The infinite sum in (3.4) is of course truncated to some window W as discussed in refs. [4, 10]. The error σ_χ, corrected for autocorrlations, is then given by

$$\sigma_\chi^2 = \frac{\Gamma(0)}{\#\mathrm{C}} (1 + 2\varepsilon\bar{\tau}) . \tag{3.5}$$

A glance at table 1 shows that the factor in brackets in eq. (3.5), which corrects the naive error estimate, does not grow large in our simulations. This error estimate was also found consistent with errors from binning, which we monitored in addition for each observable. Due to the small amplitude of the tail of the autocorrelation, it would be very wasteful not to measure each cluster in spite of the fact that they are asymptotically correlated on a time scale large compared to unity. Just because of the smallness of Γ it is rather hard – and unnecessary for the error estimate – to determine $\bar{\tau}$ accurately. Typically the window W could only be taken $2\bar{\tau} \ldots 3\bar{\tau}$ wide because of noise. One should safely allow for about 20% error for $\bar{\tau}$ in table 1. In improved estimates of short-distance quantities like the nearest-neighbor correlation no autocorrelations are detectable at all. This is rather different from standard estimators in conjunction with the cluster algorithm [3, 4]. There, short-distance quantities were harder than long-distance correlations.

It may seem that the autocorrelation time $\bar{\tau}$ is not so small. Between successive measurements, however, we perform only of order $\langle |\mathrm{C}| \rangle \cong 0.75\chi$ operations. As in ref. [4], we have to convert $\bar{\tau}$ to

$$\tau = \frac{\langle |\mathrm{C}| \rangle}{LT} \bar{\tau} = 0.75 \frac{\chi}{LT} \bar{\tau} \tag{3.6}$$

before it is comparable to "sweeps". We then derive values below one as in refs. [3, 4]. We conclude that we presumably see the same fundamental autocorrelation time as with standard estimators for the 1C algorithm. Only the amplitude is very small – which is just as important from a practical point of view as far as equilibrium measurements are concerned. If a precise determination of the relaxation time is the main objective, then standard estimators are preferable. A physical picture behind the smallness of ε is as follows: Since each estimate entirely results from the one cluster that is flipped, it takes – roughly speaking – overlapping successive clusters to get strongly correlated estimates. Each cluster starts from a random site, grows to a typical size $\langle |\mathrm{C}| \rangle$, and thus the overlap probability is controlled by $\langle |\mathrm{C}| \rangle / LT$, which is of the same order as ε.

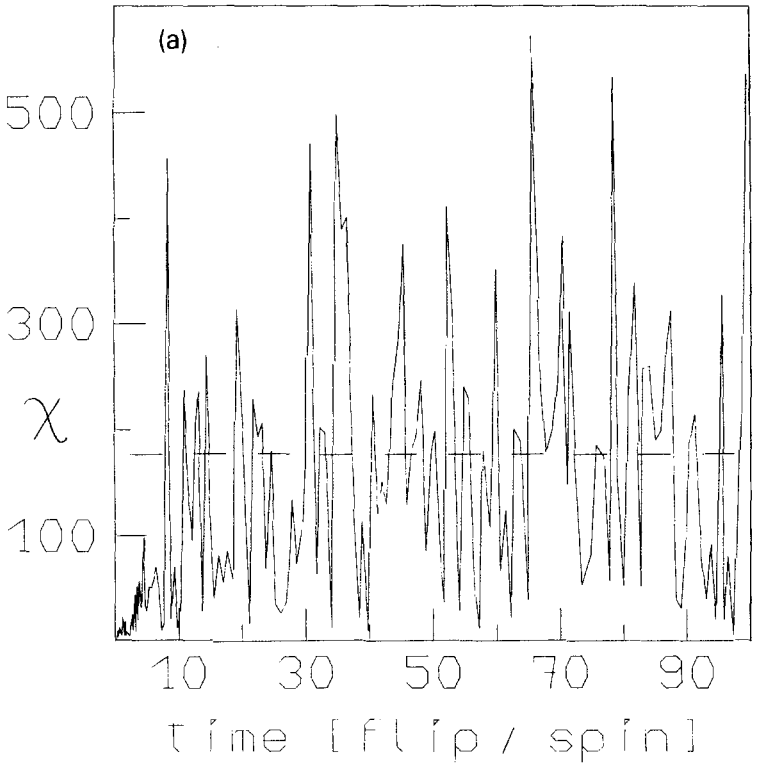

Fig. 1. (a) Equilibration of the magnetic susceptibility on 128^2 at $\beta = 1.5$ (correlation length $\cong 11$) from a "hot" start. The time unit is comparable to sweeps. The dashed line is the equilibrium average taken from a long run.

With short autocorrelation times at equilibrium we also found equilibration easy to achieve. During an equilibration run of for instance 1000τ all observables settle to fluctuate around equilibrium values, and this takes a negligible fraction of the run time. In fig. 1 we see as an example the equilibration of the 128^2 lattice at $\beta = 1.5$ from disordered and ordered starts. The standard magnetic susceptibility (left part of eq. (2.21)) is displayed as a typical observable here, and the evolution time is made comparable to "sweeps" by adding up the occurring cluster sizes and dividing by the volume as discussed after eq. (3.6).

At short distance but still in the scaling regime, i.e. for $1 \ll |x| \ll m^{-1}$, we fit the two-point function to (B.21) of appendix B. Specializing it to $n = 3$ and inserting numerical constants we thus determine $\Lambda_{\overline{\mathrm{MS}}}$ in lattice units by fitting

$$\langle \sigma_x \cdot \sigma_0 \rangle = B\left(t + \log t + 1.1159 + \frac{\log t}{t} + \frac{0.1159}{t} \right)^2, \tag{3.7}$$

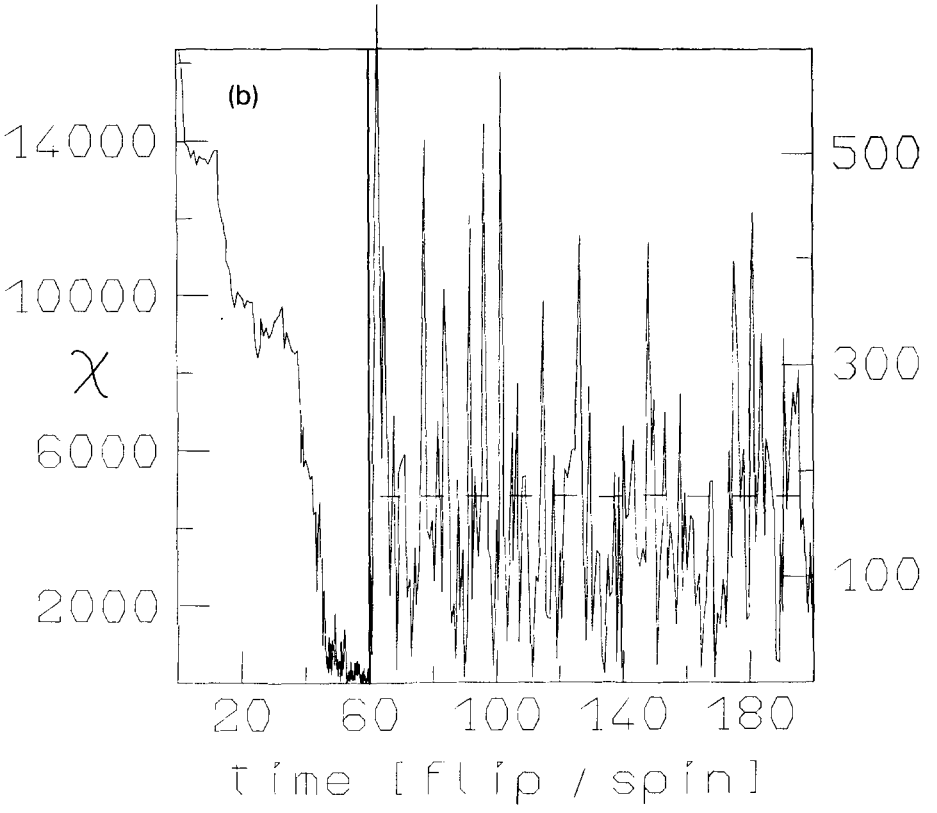

Fig. 1. (b) Same as (a) from a "cold" start. The scale of the vertical axis changes at $t = 60$.

where

$$t = -\log(\Lambda_{\overline{\mathrm{MS}}}|x|). \tag{3.8}$$

As input for these fits we measured the correlation function parallel to the spatial lattice axis at the nearest integer distances to $|x| = 2^{1/2}, 2^1, \ldots, 2^{11/2}, 2^6$. Also measured, but not used in the fit, were correlations along the lattice diagonal over distances that are larger by a factor $\sqrt{2}$. For the somewhat larger separations we get pairs of points in this way which have almost identical euclidean distances but maximally different orientation relative to the lattice axes. Their comparison is indicative for the degree of restoration of rotational invariance. For $\beta = 1.9$ we list these correlation data in table 2. Fit and data are plotted in fig. 2. For best fit parameters B, and $\Lambda_{\overline{\mathrm{MS}}}$ taken from a least-square fit, the difference between data and fit is given in multiples of the statistical error of the data at each distance $|x|$. One unit on the vertical axis corresponds to a relative discrepancy of 1×10^{-3}–2×10^{-3} depending on the distance (see table 2). We see that we obtain a rather good fit

TABLE 2
The correlation function at short distance for $\beta = 1.9$

On axis		Diagonal	
$\|x\|$	$\langle \sigma_0 \cdot \sigma_x \rangle$	$\|x\|$	$\langle \sigma_0 \cdot \sigma_x \rangle$
1	0.7072(7)		
2	0.5862(6)	1.41	0.6331(7)
3	0.5188(6)	2.83	0.5246(6)
4	0.4735(6)	4.24	0.4630(6)
6	0.4127(5)	5.66	0.4206(5)
8	0.3714(5)	8.49	0.3628(5)
11	0.3272(5)	11.3	0.3232(5)
16	0.2772(4)	15.6	0.2808(4)
23	0.2307(4)	22.6	0.2328(4)
32	0.1902(3)	32.5	0.1884(3)
45	0.1507(3)	45.3	0.1501(3)
64	0.1129(2)	63.6	0.1135(2)

from $|x| = 45$ ($\simeq 1/3$ of the nonperturbative correlation length) down to a few lattice spacings along the axis. For $|x| \geqslant 8$ coincidence between rotationally invariant fit and both on-axis and diagonal data is better than 10^{-3}. The clearly visible discrepancies at very short distance are actually rather small on the scale $1/|x|^2$ expected for lattice artifacts. The matching of the fit below the one-σ level in the medium range of fig. 2 shows that, of course, data at various separations coming from the same configurations (clusters) are not independent. Beyond $|x| = 45$ the data abruptly break away from the perturbative formula with on-axis and diagonal points staying together. This, of course, has to be the case, as the correlation can

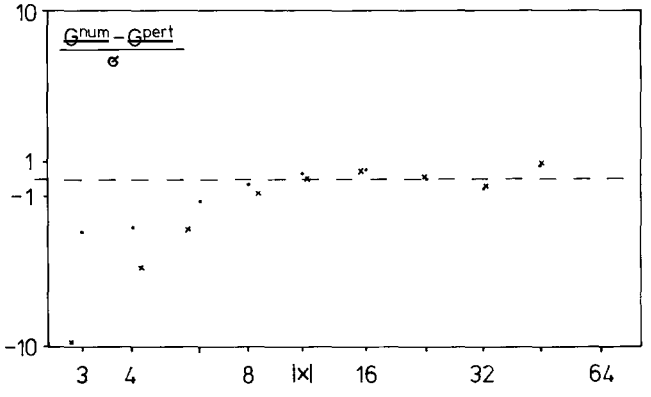

Fig. 2. Difference between the numerical two-point function for $\beta = 1.9$ (see table 2) and a fit to the perturbative form (3.7) in units of the statistical errors which correspond to an accuracy of 1×10^{-3}–2×10^{-3}. The dots are on-axis correlations, and crosses denote correlations along the lattice diagonal.

TABLE 3
Perturbative energy scale $\Lambda_{\overline{\rm MS}}$ in lattice units with statistical errors, range of on-axis separations where it is fitted, and ratio of long-to-short distance scale with an estimate of systematic errors

β	Range	$\Lambda_{\overline{\rm MS}}$	$m/\Lambda_{\overline{\rm MS}}$
1.9	$8 \to 32$	0.00321(1)	2.55(10)
1.8	$6 \to 23$	0.00611(1)	2.53
1.7	$4 \to 11$	0.01169(2)	2.48

become nonperturbative, but it has to stay rotationally symmetric until it feels the rectangular shape of the torus. The breakaway is clearly caused by t in the perturbative formula (3.7) not being large anymore. The bare correlation $\langle \sigma_x \cdot \sigma_0 \rangle$ decays smoothly with $|x|$. In table 3 results from similar fits for various β-values are listed. The second column gives the range of on-axis correlations used in the fit, and in the next column the resulting $\Lambda_{\overline{\rm MS}}$ in lattice units follows. There the quoted errors are purely statistical, i.e. we pretended that (3.7) is exact and only analyzed by binning how well $\Lambda_{\overline{\rm MS}}$ is fixed by the data. Since in the fitted range t is not really very large (2...4), it is likely, however, that the systematic error coming from our ignorance of higher-order perturbative terms is much more important. To estimate it we report on a number of additional experiments with the $\beta = 1.9$ data and indicate the level of changes of $\Lambda_{\overline{\rm MS}}$ in parentheses. We first moved the fit window by one (measured) point in either direction (1/2%). Then, according to (B.21), we optimized the scheme parameter c leading to $c = 0.28$ and reconverted the obtained value for $\Lambda_{\rm c}$ to $\Lambda_{\overline{\rm MS}}$ (1%). Finally, we added a term $-\log^2(t)/(2t^2)$ under the bracket in (3.7). This is the next term in (B.18), and we hope that it gives us a feeling for possible effects of the next order in perturbation theory (3%). This type of uncertainty is used as an error estimate for the ratio $m/\Lambda_{\overline{\rm MS}}$ in the last column of table 3. For QCD practitioners we add that the MS-scheme corresponds to $c = -0.97$. This value leads to a rather vigorous resummation of the perturbation series in a direction opposite to scheme optimization. A fit in the MS-scheme leads to a 10% larger value for $\Lambda_{\overline{\rm MS}}$. For a pessimistic estimate one should perhaps also allow for errors of this size. At smaller β the window, where a fit of the short-distance continuum behavior is possible, shrinks. However, using our experience from $\beta = 1.9$ that on-axis correlations show little lattice artifacts, we may shift the fit window downward and obtain the remaining lines of table 3. We regard this as reasonable scaling behavior as the correlation length changes by a factor of ≈ 4. One should, of course, be aware of the fact that systematic errors from higher-order terms scale, too, under this procedure. Thus stability does not necessarily imply accuracy. Also, for the desired ratio $m/\Lambda_{\overline{\rm MS}}$, one in principle has to extrapolate the masses of table 1 from finite to infinite L. For the O(3)-model at hand this is possible without further parameters on the basis of Lüscher's formula [11]. For

$\beta = 1.9$ and $L = 512$ we find a 1% change to $m_\infty^{-1} = 122.5$, which is included in table 3, and changes for the other simulations are negligible. Clearly, in view of the uncertainties in $\Lambda_{\overline{\rm MS}}$, statistical and systematic errors in m are immaterial.

4. The mass gap in a small volume

Lüscher [5] has pioneered the method of using finite volume effects as probes for universal physics in asymptotically free theories. In particular, if the length scale L given by the spatial volume is smaller than or perhaps comparable to the inverse mass gap of the transfer matrix $m^{-1}(L)$, a relation between the three scales $m, L, \Lambda_{\overline{\rm MS}}$ can be derived by renormalized perturbation theory. For the O(n) σ-models the relation reads

$$\frac{m(L)}{\Lambda_{\overline{\rm MS}}} = \frac{\mathrm{e}^{-\Gamma'(1)}}{4\pi}\left(\frac{n-2}{\pi(n-1)}\right)^{1/(n-2)} (z\,\mathrm{e}^{\pi/z})^{(n-1)/(n-2)}\big(1 + a_1 z + \mathrm{O}(z^2)\big), \quad (4.1)$$

where the dimensionless expansion parameter is

$$z = Lm(L). \quad (4.2)$$

The leading terms in eq. (4.1) have been calculated as infinite cut-off limits in dimensional regularization [5] and on the lattice [12]. Floratos and Petcher [13] report the value

$$a_1 \cong 0.32/(n-1) \quad (4.3)$$

for the order z correction. Their calculation is at two-loop order but requires knowledge of the three-loop β-function [14].

We shall use eq. (4.1) together with a lattice simulation to find the lattice spacing in physical units that corresponds to certain values β of the bare inverse coupling. More precisely, for $n = 3$, we solve eq. (4.1) for the Λ-parameter

$$\Lambda_{\overline{\rm MS}}^{-1} \cong m(L)^{-1}\,\frac{\mathrm{e}^{-\Gamma'(1)}}{8\pi^2}\mathrm{e}^{2\pi/z}z^2(1 + a_1 z), \quad (4.4)$$

with m and $\Lambda_{\overline{\rm MS}}$ in lattice units. For large enough β ($\beta = 1.9$ for instance), one hopes to find a range of L where the right-hand side of (4.4) is approximately L-independent and yields a good estimate of $\Lambda_{\overline{\rm MS}}$. This range is restricted by two different effects. If L grows at fixed β we leave the small volume domain and z grows beyond order one. Eventually it will even diverge as $m(L)$ saturates at the infinite volume value. Since we know only a few terms of an asymptotic small z expansion, we cannot expect a decent approximation beyond $z \leqslant \mathrm{O}(1)$, and it may

TABLE 4
Inverse mass gaps m^{-1} in small volumes

L	$\beta = 1.7$	$\beta = 1.8$	$\beta = 1.9$
8			9.80(2)
12	10.84(2)	12.38(3)	13.80(3)
16	13.38(3)	15.52(4)	17.60(4)
18	14.55(4)		
20	15.68(4)	18.54(5)	21.02(5)
22	16.71(5)		
24	17.68(5)	21.13(5)	24.34(6)
26	18.58(8)		
28	19.54(5)	23.69(6)	27.44(7)
32	21.13(6)	26.14(6)	30.49(7)
64		41.3(2)	51.1(3)

even have to be rather small. At small L the cutoff given by the lattice spacing becomes comparable to our physical scales, and lattice artifacts are important.

Results for the inverse mass gap $m^{-1}(L)$ for some L and three different β are listed in table 4. Most of these results stem from runs with $T = 512$. Only in some cases older runs with $T = 128$ or 256 were also taken into account after ascertaining the absence of systematic differences. Again, only time separations larger than $2m^{-1}(L)$ entered into fits. The plot in fig. 3 exhibits the finite volume data in a direct fashion without further theoretical input. It shows good scaling behavior as data from $\beta = 1.7, 1.8, 1.9$ have been combined.

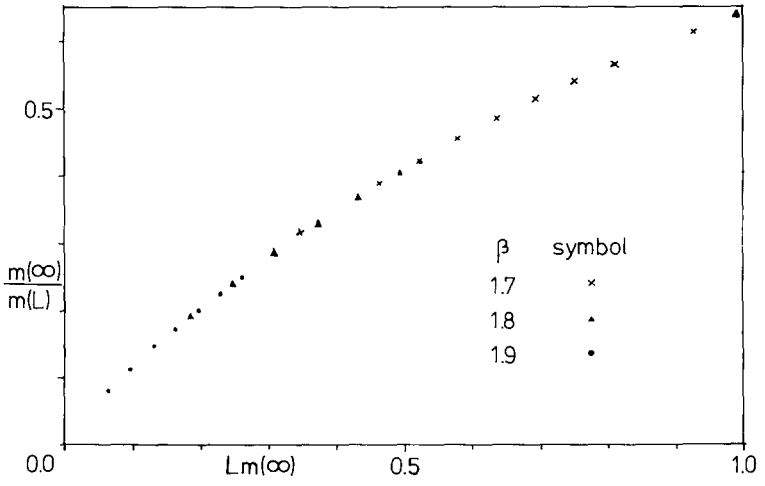

Fig. 3. Finite volume mass gap scaling behavior (see table 4).

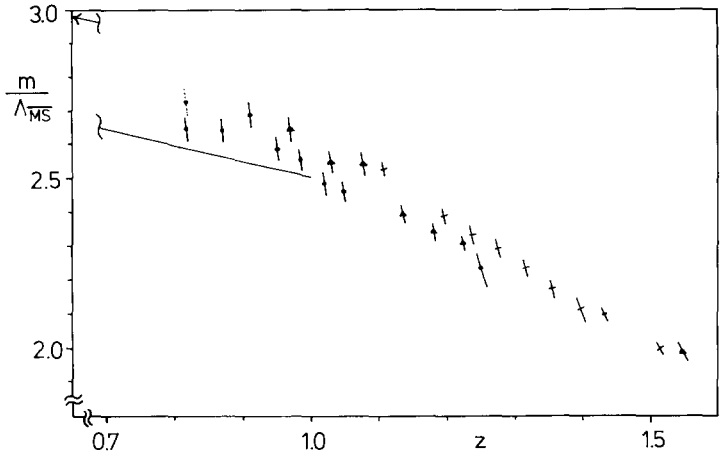

Fig. 4. Infinite volume mass gap in units of the perturbative scale $\Lambda_{\overline{\mathrm{MS}}}$ which in turn is derived from the finite volume mass gap. Errors are 2σ.

In fig. 4 we combine the small volume data, (4.4) without the $a_1 z$ term, and the large volume masses from table 1 (extrapolated to $L = \infty$ [11]) to plot $m(\infty)/\Lambda_{\overline{\mathrm{MS}}}$ versus z. It is perhaps not superfluous to emphasize the distinct nature of this plot from those found in refs. [5, 6, 13], where the authors try to extrapolate $m(L)/\Lambda_{\overline{\mathrm{MS}}}$ to $z \to \infty$. The basically small errors of $m(L)$ are strongly amplified in fig. 4 by z entering as exponent into the theoretical formula, and much more fine structure is exhibited than in fig. 3, where symbols are larger than errors. Data points belonging to the same β-value can be joined by smooth curves if the errors are taken into account. These curves, however, seem to systematically come down with β by margins above our errors. This tendency is stronger at small z which means smaller L. This suggests non-universal finite lattice spacing effects as a possible origin. Close to $z = 1$, for example, there are two nearby data points from $\beta = 1.9$ and $L = 28$, and from $\beta = 1.8$ and $L = 16$. From the finite lattice calculation in ref. [12], the one-loop lattice perturbation theory contribution to the finite L effects can be extracted. It lifts the $L = 12$ points by 1.3%, and the correction for other L follows from its being proportional to L^{-2}. For $\beta = 1.9$, $L = 8$, the dotted bar shows the data point corrected by 3%. We must conclude that the one-loop finite lattice spacing correction has the wrong sign to explain the non-universality that we see. The inadequacy of one-loop lattice perturbation theory may perhaps not be too surprising. The leading term $m^{-1}(L) \cong \beta L$ has to be lowered by almost a factor two by the $1/\beta$ corrections. While one expects that the resummation in terms of renormalized quantities like in eq. (4.1) leads to better convergence, it is not clear in general how well non-universal corrections are represented by the lowest order.

In the absence of a quantitative handle on the finite L corrections, we could not think of an entirely convincing way to extrapolate to $z = 0$. The line in fig. 4

extrapolates the point (1.0, 2.5) that is suggested by the $\beta = 1.9$ data at not too small L, using the value $a_1 = 0.16$ of ref. [13]. It ends at $m/\Lambda_{\overline{\rm MS}} \cong 3$. The slope is roughly consistent with the data.

5. Scaling with the bare lattice coupling

For large values of the inverse bare lattice coupling β all physical quantities in asymptotically free theories can be related to a renormalization group invariant energy scale $\Lambda(\beta)$ defined as a solution of

$$\left(1 + B(\beta)\frac{\partial}{\partial\beta}\right)\Lambda(\beta) = 0. \tag{5.1}$$

Here Λ is in lattice units, and the lattice beta function $B(\beta)$ has a perturbative expansion

$$B(\beta) = \sum_{i=0}^{\infty} B_i \beta^{-i}. \tag{5.2}$$

The first two universal coefficients are identical to those in any perturbative renormalization scheme (see eq. (B.3)),

$$B_0 = (n-2)/2\pi, \qquad B_1 = (n-2)/(2\pi)^2, \tag{5.3}$$

and the non-universal three-loop coefficient for the standard lattice action is reported in ref. [15] to be

$$B_2 = \left[(n-2)/(2\pi)^3\right] h, \qquad h = 0.516 - 0.086(n-2). \tag{5.4}$$

The solution to eq. (5.1) with the standard choice for the integration constant is

$$\Lambda = \Lambda_{\rm L}\lambda, \tag{5.5}$$

with

$$\Lambda_{\rm L} = {\rm e}^{-\beta/B_0}(\beta/B_0)^{B_1/B_0^2} \tag{5.6}$$

and

$$\lambda = \exp\left\{\int_{\beta}^{\infty} {\rm d}u \left(\frac{1}{B(u)} - \frac{1}{B_0} + \frac{B_1}{B_0^2 u}\right)\right\}. \tag{5.7}$$

In the three-loop approximation we thus have for the O(3)-model

$$\Lambda = {\rm e}^{-2\pi\beta} 2\pi\beta\left[11 + (1-h)/2\pi\beta + {\rm O}(1/\beta^2)\right]. \tag{5.8}$$

TABLE 5
Results for nearest neighbor correlation E, and ratio of scales $m/\Lambda_{\overline{\rm MS}}$ converted after evaluation with the lattice Λ-parameter in various approximations. Errors in the last column reflect the effect of the uncertainty in E when used in eq. (5.21)

β	E	Two-loop	Three-loop	(5.19)
1.4	0.5620(1)	4.00	3.76	2.03
1.5	0.6016(2)	4.36	4.11	2.42
1.6	0.6359(3)	4.45	4.22	2.71
1.7	0.6634(3)	4.33	4.12	2.80
1.8	0.6878(3)	4.09	3.90	2.82(1)
1.9	0.7072(7)	3.84	3.67	2.74(3)

A physical energy, as for instance the mass gap m, is expected to tend to a constant multiple of Λ for $\beta \to \infty$. This behavior should be accelerated by inclusion of the three-loop term in $\lambda \neq 1$. The Λ-parameters of different renormalization schemes can be related in the cut-off limit. In particular, it is known that

$$\Lambda_{\rm L}/\Lambda_{\overline{\rm MS}} = 32^{-1/2} \exp\left[-\frac{\pi}{2(n-2)} \right] \tag{5.9}$$

holds for the O(n) σ-model [5]. We combine eqs. (5.8) and (5.9) with our data on mass gaps for infinite volumes to compile table 5 with estimates $m/\Lambda_{\overline{\rm MS}}$. It is evident that these values are by no means β-independent, not even monotonic if we include $\beta \leqslant 1.6$. This may explain some of the confusion about this quantity. The suspicion that some coefficients of higher orders in $1/\beta$ in eq. (5.8) cannot be small is confirmed. Moreover, the values $m/\Lambda_{\overline{\rm MS}}$ in table 5 are about 30–50% higher than those derived from more physical quantities in tables 3 and 4. It may, however, also be noted that the tendency beyond $\beta = 1.6$ and also the $1/\beta^2$ term in λ work at least in the right direction. Nevertheless, asymptotic scaling in the bare coupling with the standard lattice action is far away even at correlation lengths around 100.

We now present a semi-phenomenological form of the lattice β-function that is more successful with regard to scaling. In ref. [16] an observable was introduced which is closely related to coupling constant renormalization in the background field definition. It makes use of the generators J^{ij}, $i<j=1,\ldots,n$ of the SO(n) symmetry of the σ-model, that act on the same Hilbert space as the transfer matrix $\exp(-H)$ and generate global rotations in the i–j plane of spin space. In ref. [16] (see also ref. [4] for $n=2$) it was shown that the thermal expectation value of the SO(n)-Casimir operator is given by simple euclidean observables,

$$\left\langle \sum_{i<j} (J^{ij})^2 \right\rangle = \frac{\mathrm{Tr}\left(\mathrm{e}^{-TH} \sum_{i<j} (J^{ij})^2 \right)}{\mathrm{Tr}\, \mathrm{e}^{-TH}} = (n-1)(\beta E - C)\,. \tag{5.10}$$

Here E is the nearest neighbor correlation in time direction,

$$E = (L/T)\langle \sigma_x \cdot \sigma_{x+\hat{2}} \rangle , \tag{5.11}$$

and C [16] is the susceptibility of the Noether current

$$C = \frac{\beta^2}{(n-1)T^2} \sum_{i<j} \left\langle \left(\sum_x \sigma_x \cdot t^{ij} \sigma_{x+\hat{2}} \right)^2 \right\rangle . \tag{5.12}$$

In eq. (5.12) t^{ij} are the real antisymmetric $n \times n$ matrix generators of SO(n). The hamiltonian H and Casimir-operator $\Sigma (J^{ij})^2$ may be diagonalized simultaneously in a basis $|k\rangle$ with eigenvalues ε_k and q_k^2. We then have

$$\left\langle \sum_{i<j} (J^{ij})^2 \right\rangle = \frac{\Sigma_k \mathrm{e}^{-T\varepsilon_k} q_k^2}{\Sigma_k \mathrm{e}^{-T\varepsilon_k}} \equiv Q^2 , \tag{5.13}$$

which shows that Q^2 is a dimensionless physical quantity: A combination of energies of low-lying states and the inverse physical temperature in lattice units T with group-theoretically fixed coefficients. We may thus control the scaling limit by keeping Q^2 fixed when β and L, T (L/T also fixed) diverge. We now specialize to $L = T$. If Q^2 is not small but kept fixed at a value of O(1), then it is clear from eq. (5.13) that we are taking a scaling limit at physically small volume with size and temperature comparable to the mass gap. This is quite similar to Lüscher's small volume mass gap [5]. We just do not have to isolate the lowest excitation, and therefore Q^2 is an "easier" quantity. It will be interesting to study it numerically in more detail (with the new algorithm) than it was possible in ref. [15].

Here we just want to use Q^2 to derive the lattice β-function from

$$\left(L\frac{\partial}{\partial L} + B(\beta)\frac{\partial}{\partial \beta} \right) Q^2 = 0 . \tag{5.14}$$

Using eq. (5.10) it is given by

$$B(\beta) = L\frac{\partial C}{\partial L} \Big/ \left(\frac{\partial}{\partial \beta}(\beta E) - \frac{\partial C}{\partial \beta} \right) , \tag{5.15}$$

where we used the fact that E becomes L-independent for large L. The perturbative expansion of E is easily derived to second order.

$$E = 1 - (n-1)/4\beta - (n-1)/32\beta^2 + \mathrm{O}(1/\beta^3) , \tag{5.16}$$

and for C we introduce

$$C = C_0(L) + C_1(L)/\beta + O(1/\beta^2). \tag{5.17}$$

If we expand eq. (5.15) in $1/\beta$, we find the universal terms of the β-function given by the logarithmic divergencies in C_0 and C_1,

$$B_{0,1} = \lim_{L\to\infty} L\frac{\partial C_{0,1}}{\partial L}, \tag{5.18}$$

and the one-loop term has been computed in this way in ref. [16]. It matched numerical results for C rather well at larger β. We now make the crucial observation that in the two-loop approximation underlying the search for asymptotic scaling, the term $\partial/\partial\beta(\beta E)$ is replaced by 1 as it is formally of order $1/\beta^2$. If on the other hand, we estimate it between $\beta = 1.8$ and 1.9 from the data for E in table 5, we find it quite comparable to the two-loop $1/\beta$ term from C_1. We are thus motivated to keep part of the higher-order terms in eq. (5.15) and use the approximation

$$\tilde{B}(\beta) = (B_0 + B_1/\beta)\left(\frac{\partial}{\partial\beta}\beta E\right)^{-1}. \tag{5.19}$$

Inserting $\tilde{B}$ in eq. (5.7) leads to

$$\log\tilde{\Lambda} = \int_\beta^\infty \mathrm{d}u\left[\frac{\partial}{\partial u}uE(u) - 1\right]\left(\frac{1}{B_0} - \frac{B_1}{B_0^2 u}\right), \tag{5.20}$$

The integration can partly be carried out,

$$\log\tilde{\Lambda} = \frac{1}{B_0}\left\{-\frac{n-1}{4} + \beta(1-E(\beta)) - \frac{B_1}{B_0}\int_\beta^\infty \mathrm{d}u\,\frac{E(u)+uE'(u)-1}{u}\right\}. \tag{5.21}$$

The first terms lead to $\tilde{\Lambda} = 1.42$ at $\beta = 1.9$, a rather sizeable correction. The term with the remaining integral requires knowledge of $E(u)$ at large β. Here we used the mean-field approximation of ref. [16] which reproduces the numerical value at $\beta = 1.8$ with an accuracy of better than 1%. Moreover, if one expands the saddle point equation for large β, one recovers the perturbative terms in eq. (5.16). The leading mean-field approximation for E can easily be refined, but we found it sufficient to evaluate numerically the second term in eq. (5.21). It lowers $\tilde{\Lambda}$ at $\beta = 1.9$ by about 5% and thus preserves the main effect. The last column in table 5 quotes $m/\Lambda_{\overline{\mathrm{MS}}}$ with the β-function $\tilde{B}$ including both terms in eq. (5.21). We find these values much more stable and more consistent with our other results.

Although the preceding result, that the nearest neighbor correlation contains a lot of information about lattice artifacts that can be corrected for, is pleasant, we must point out a consistency problem here. Our approximation $\tilde{B}$ in eq. (5.19) contains the correct universal terms and also a certain three-loop term $-B_0(n-1)/(32\beta^2)$. It differs from eq. (5.4) by the sign and a factor of 5 in magnitude for $n=3$. The success of $\tilde{B}$ would be more plausible, if it approximately contained the correct three-(and higher) loop terms. Any attempt to simply add a $1/\beta^2$ term to $\tilde{B}$ to fix the discrepancy led to bad scaling behavior. In our opinion, it would be very desirable to perform a second independent calculation of B_2. Starting from eq. (5.15) this may even be possible directly on the lattice, as we do not need any wavefunction renormalization factors. This is the typical efficiency of background field techniques [17]. To conclude, we suggest, even in the absence of a foundation like eq. (5.10), to try to use the mean plaquette in lattice gauge theory to phenomenologically improve scaling in a similar way as in the present study of the O(3)-model.

Note added

After completion of this work the author learned of ref. [22], where the internal energy is used to improve asymptotic scaling in a similar spirit.

6. Conclusions

In our new application we found the collective Monte Carlo algorithm to work as well in the nonabelian O(3) σ-model as it did in the x–y model. Critical slowing down did not pose any problems in these studies. Variance reduction by improved estimators led to a further significant gain in efficiency, at least for the two-point function. Apart from equilibration, the lattice may be enlarged at no cost other than memory if the correlation length stays fixed. This is due to the fact that with improved estimators and collective updating it is the correlation volume which determines the average number of operations necessary for an estimate of the correlation function at all distances. With more fast computer memory available one could envisage the simulation of spin systems yet closer to criticality than in this study or in ref. [4].

We concentrated on the ratio $m/\Lambda_{\overline{\mathrm{MS}}}$ in investigating the physics of the O(3)-model. Three different methods led us to values between 2.5 and 3. In particular, we saw the two-point function assume its universal perturbative form in x-ranges simultaneously smaller than the correlation length but much larger than the lattice spacing. As a byproduct the rotational invariance of the two-point function showed up in a very direct fashion. The small volume method remained somewhat inconclusive, since even below $z=1$ the extrapolation to $z=0$ is not easy, and the method as applied here becomes extremely sensitive to errors in $m(L)$. A more or less

horizontal extrapolation of the smallest z data in fig. 4 would be more consistent with our remaining results but in conflict with ref. [13]. Intriguingly good results were obtained with an approximate lattice β-function that uses information on the nearest neighbor correlation to correct for higher-order non-universal terms.

We think that we have confirmed with the study in this paper and ref. [4] how important it is to develop improved algorithms and tools rather than just relying on ever faster and bigger computers. In two-dimensional models we probed a new domain of couplings where the spin systems are much closer to criticality or field theoretic behavior than in past studies. Further qualitatively new questions can be tackled in the future. The lesson concerning four-dimensional nonabelian gauge theory is in our opinion that present day data should be judged with great care. One should from time to time ask oneself what one could and would conclude about the σ-model at similar lattice size, correlation length and statistics. Clearly the development of a comparable collective algorithm for gauge fields is an important goal now. As fast computer memory will become more amply available in the near future we could then very significantly boost our understanding of realistic quantum field theories beyond perturbation theory.

I would like to thank Martin Lüscher for discussions and advice at every stage of this work and for making ref. [12] available to me. The simulations were carried out on the Cray X-MP/216 at Kiel University.

Appendix A

CORRELATION FUNCTION IN PERTURBATION THEORY

In this appendix we compute the renormalized two-point function of the O(n) σ-model in the two-loop approximation. Using the position space dimensional regularization technique (DR) of ref. [18], we take particular care to correctly identify the x-independent constants in the correlation function which set the scale of the logarithms. For the same reason we introduce a magnetic field as infrared regulator which is sent to zero only after renormalization in the minimal subtraction scheme. An analogous computation for the SU(n) × SU(n) matrix model, from which the present calculation is largely plagiarized, can be found in ref. [12]. The standard parametrization for the perturbative expansion of the σ-model is

$$\sigma(x) = \left(\left(1 - \pi^2(x)\right)^{1/2}, \pi(x)\right), \tag{A.1}$$

where the bare field $\pi(x)$ has $n - 1$ real components which are always appropriately

contracted. The expansion is generated by the action

$$S(\pi)=\frac{1}{2g_0^2}\int \mathrm{d}^D x\left\{(\partial\pi)^2+\frac{(\partial\pi^2)^2}{4(1-\pi^2)}-2h_0(1-\pi^2)^{1/2}\right\}, \tag{A.2}$$

where $x=(x_1, x_2, y_1, \ldots, y_{D-2})$ is the D-dimensional extension of the position $x=(x_1, x_2)$, and ∂ in eq. (A.2) is the corresponding derivative. Contact terms arising from the measure on the sphere are regularized to zero in DR. We implement the renormalization program by eliminating bare parameters by

$$g_0^2=\mu^\varepsilon g^2 Z_1 \tag{A.3}$$

and

$$h_0=hZ_1Z^{-1/2}, \tag{A.4}$$

with $\varepsilon=2-D$, and the renormalized two-point function then reads

$$G(x)=\int \mathrm{d}^{D-2}y Z^{-1}\langle(1-\pi^2(0))^{1/2}(1-\pi^2(x))^{1/2}+\pi(0)\pi(x)\rangle. \tag{A.5}$$

The unphysical components y of x are integrated over which corresponds to vanishing unphysical momenta [18]. The correlation G will be finite for $\varepsilon\to 0$ with appropriate MS renormalization constants

$$Z=1+g^2Z^{(1)}+g^4Z^{(2)}+\ldots \tag{A.6}$$

and

$$Z_1=1+g^2Z_1^{(1)}+\ldots. \tag{A.7}$$

After rescaling $\pi\to g_0\pi$ we expand the action as $S=S_0+g^2S_1+\ldots$ with

$$S_0=\tfrac{1}{2}\int \mathrm{d}^D\pi(-\partial^2+h)\pi \tag{A.8}$$

and

$$S_1=\tfrac{1}{2}\int \mathrm{d}^D x\left\{h\left(Z_1^{(1)}-\tfrac{1}{2}Z^{(1)}\right)\pi^2+\tfrac{1}{4}h\mu^\varepsilon(\pi^2)^2+\tfrac{1}{4}\mu^\varepsilon(\partial\pi^2)^2\right\}. \tag{A.9}$$

We further obtain

$$\begin{aligned} G(x)&\cong 1+g^2G_1(x)+g^4G_2(x)\\ &=Z^{-1}\int \mathrm{d}^{D-2}y\langle 1+g^2O_1(x)+g^4O_2(x)\rangle, \end{aligned} \tag{A.10}$$

with

$$O_1(x) = \mu^{\varepsilon}\big(\pi(x)\pi(0) - \pi^2(0)\big), \tag{A.11}$$

$$O_2(x) = Z_1^{(1)} O_1(x) + \tfrac{1}{4}\mu^{2\varepsilon}\Big\{\pi^2(x)\pi^2(0) - \big(\pi^2(0)\big)^2\Big\}. \tag{A.12}$$

The average with the full action reduces to $\langle \dots \rangle_0$ with S_0 only in

$$G(x) \cong Z^{-1}\int \mathrm{d}^{D-2}y\,\big\{1 + g^2\langle O_1\rangle_0 + g^4\big(\langle O_2\rangle_0 - \langle O_1 S_1\rangle_0^{\mathrm{c}}\big)\big\}. \tag{A.13}$$

We now evaluate

$$\begin{aligned} G_1(x) &= \int \mathrm{d}^{D-2}y\,\big[-Z^{(1)} + \langle O_1(x)\rangle_0\big] \\ &= \int \mathrm{d}^{D-2}y\big[-Z^{(1)} + \mu^{\varepsilon}(n-1)\big(D(x) - D(0)\big)\big] \end{aligned} \tag{A.14}$$

with the D-dimensional propagator

$$\begin{aligned} D(x) &= \int_0^{\infty}\mathrm{d}t \int \frac{\mathrm{d}^D p}{(2\pi)^D}\mathrm{e}^{-t(p^2+h)+ip\cdot x} \\ &= \int_0^{\infty}\mathrm{d}t\,(4\pi t)^{-D/2}\mathrm{e}^{-th - x^2/4t} \end{aligned} \tag{A.15}$$

solving

$$(-\partial^2 + h)D(x) = \delta^D(x). \tag{A.16}$$

With $\int \mathrm{d}^{D-2}y = 1 + \mathrm{O}(\varepsilon)$ [18] we get

$$\begin{aligned} G_1(x) &= \int \mathrm{d}^{D-2}y\left[-Z^{(1)} - \frac{n-1}{4\pi}\big(4\pi\mu^2/h\big)^{\varepsilon/2}\Gamma(\varepsilon/2)\right] \\ &\quad + \frac{n-1}{2\pi}\mu^{\varepsilon}K_0\big(h^{1/2}|x|\big) \\ &\xrightarrow{\varepsilon\to 0} \frac{n-1}{2\pi}\left\{K_0\big(h^{1/2}|x|\big) - \frac{1}{2}\log\big(4\pi\mu^2/h\big) - \frac{1}{2}\Gamma'(1)\right\}, \end{aligned} \tag{A.17}$$

provided we insert the well-known result

$$Z^{(1)} = -\frac{n-1}{2\pi}\frac{1}{\varepsilon}. \tag{A.18}$$

Using an expansion for the Bessel function $K_0(z) \simeq -\log(z/2) + \Gamma'(1)$ as $z \to 0$ we can now turn off the magnetic field h and we are left with

$$G_1(x) = \frac{n-1}{2\pi}\left\{-\log(\mu|x|) + \frac{1}{2}\Gamma'(1) - \frac{1}{2}\log\pi\right\}. \tag{A.19}$$

In the next order we obtain

$$G_2(x) = \left[(Z^{(1)})^2 - Z^{(2)}\right]\int \mathrm{d}^{D-2}y + \left(Z_1^{(1)} - Z^{(1)}\right)\left\{G_1(x) + Z^{(1)}\int \mathrm{d}^{D-2}y\right\}$$

$$+ \int \mathrm{d}^{D-2}y\left(\langle O_2(x)\rangle_0 - Z^{(1)}\langle O_1(x)\rangle_0 - \langle O_1(x)S_1\rangle_0^{\mathrm{c}}\right). \tag{A.20}$$

The gaussian expectations lead to

$$\langle O_2(x)\rangle_0 - Z^{(1)}\langle O_1(x)\rangle_0 = \tfrac{1}{2}\mu^{2\varepsilon}(n-1)\left\{[D(x)]^2 - [D(0)]^2\right\} \tag{A.21}$$

and

$$\langle O_1(x)S_1\rangle_0^{\mathrm{c}} = \mu^{2\varepsilon}(n-1)D(0)(D(x) - D(0))$$

$$+ (n-1)h\left[\mu^{\varepsilon}\left(Z_1^{(1)} - \tfrac{1}{2}Z^{(1)}\right) + \mu^{2\varepsilon}D(0)(n-3)/2\right]$$

$$\times \int \mathrm{d}^D z\left\{D(z-x)D(z) - [D(z)]^2\right\}, \tag{A.22}$$

where we also used eq. (A.16) and put $\delta^D(0) = 0$ (DR). With eq. (A.15) we integrate

$$\int \mathrm{d}^{D-2}x \int \mathrm{d}^D z\, D(z-x)D(z) = \frac{1}{4\pi}\frac{|x|}{h^{1/2}}K_1\left(h^{1/2}|x|\right) \tag{A.23}$$

and

$$\int \mathrm{d}^D z\,[D(z)]^2 = \frac{1}{4\pi h}(4\pi/h)^{\varepsilon/2}\Gamma(1+\varepsilon/2). \tag{A.24}$$

Cancelling all divergencies by the choices

$$Z^{(2)} = (n-1)\left(n-\tfrac{3}{2}\right)/(2\pi)^2\varepsilon^2, \qquad Z_1^{(1)} = -(n-2)/2\pi\varepsilon, \tag{A.25}$$

the second-order term can be written for $\varepsilon \to 0$ as

$$G_2(x) = \frac{1}{2(n-1)}\left[G_1(x)\right]^2 - \frac{(n-1)}{(4\pi)^2}(n-3)\left[\tfrac{1}{2}\Gamma'(1) + \tfrac{1}{2}\log(4\pi\mu^2/h)\right]$$

$$\times\left[h^{1/2}|x|K_1(h^{1/2}|x|) - 1\right]. \tag{A.26}$$

As expected the limit $h \to 0$ exists and leaves us with the simple form

$$G_2(x) = \left[G_1(x)\right]^2/2(n-1), \tag{A.27}$$

and

$$G(x) = 1 + \frac{g^2}{2\pi}(n-1)[-\log(\mu|x|) + a] + \frac{g^4}{8\pi^2}(n-1)[-\log(\mu|x|) + a]^2 + \mathrm{O}(g^6) \tag{A.28}$$

with

$$a = \tfrac{1}{2}(\Gamma'(1) - \log\pi). \tag{A.29}$$

We wish to remark that eq. (A.28) has also been derived with a finite volume as infrared regulator [19]. In ref. [20] no explicit infrared cutoff is introduced. The absorption of the surface of the sphere S_D into the bare coupling in ref. [20] corresponds to a finite renormalization of μ. If one takes this into account, then the result agrees with ours, too.

Appendix B

INTEGRATION OF THE RENORMALIZATION GROUP EQUATION

In appendix A we computed the renormalized two-point correlation $G = G(\mu x, g^2)$ of the O(n) σ-model in the minimal subtraction scheme up to order g^4. It has to fulfill the renormalization group (RG) equation

$$\left[\mu\frac{\partial}{\partial\mu} + \beta(g^2)\frac{\partial}{\partial g^2} + \gamma(g^2)\right]G(\mu x, g^2) = 0. \tag{B.1}$$

The β- and γ-functions are known to the three leading orders in the MS-scheme [14],

$$\beta(g^2) = -g^4(b_0 + b_1 g^2 + b_2 g^4) + \mathrm{O}(g^{10}) \tag{B.2}$$

with

$$b_0 = \frac{n-2}{2\pi}, \qquad b_1 = \frac{n-2}{(2\pi)^2}, \qquad b_2 = \frac{(n-2)(n+2)}{4(2\pi)^3}, \tag{B.3}$$

and

$$\gamma(g^2) = g^2(\gamma_0 + \gamma_2 g^4) + O(g^8) \tag{B.4}$$

with

$$\gamma_0 = \frac{n-1}{2\pi}, \qquad \gamma_2 = \frac{3(n-1)(n-2)}{4(2\pi)^3}. \tag{B.5}$$

We use eq. (B.1) as usual to relate changes in the scale μ to changes in the coupling constant g^2,

$$G(\mu x, g^2) = \exp\left\{ \int_{g^2}^{\bar{g}^2} \mathrm{d}u \, \frac{\gamma(u)}{\beta(u)} \right\} G(1, \bar{g}^2), \tag{B.6}$$

where $\bar{g}^2$ is implicitly fixed by

$$\int_{g^2}^{\bar{g}^2} \frac{\mathrm{d}u}{\beta(u)} = -\log(\mu x). \tag{B.7}$$

In eq. (B.7) asymptotic freedom manifests itself by $\bar{g}^2 \to 0$ as $x \to 0$. The integration in eq. (B.6) is performed with eqs. (B.2)–(B.5) inserted, giving

$$\exp\left\{ \int^{\bar{g}^2} \mathrm{d}u \, \frac{\gamma(u)}{\beta(u)} \right\} \propto \left\{ s + \frac{1}{n-2} - \frac{n-4}{(n-2)^2} \frac{1}{4s} \right\}^{(n-1)/(n-2)} \left(1 + O(1/s^3)\right) \tag{B.8}$$

with

$$1/s = b_0 \bar{g}^2. \tag{B.9}$$

From eq. (A.28) we see that the MS two-point function may also be written as

$$G(1, \bar{g}^2) = (1 + a/s)^{(n-1)/(n-2)} \left(1 + O(1/s^3)\right) \tag{B.10}$$

such that

$$G(\mu x, g^2) \propto \left\{ s + \frac{1}{n-2} \left[1 + a(n-2) + \left(a - \frac{n-4}{4(n-2)} \right) \frac{1}{s} \right] \right\}^{(n-1)/(n-2)} \tag{B.11}$$

holds up to corrections of $O(\bar{g}^6)$.

Finally we introduce the RG invariant scale Λ,

$$\left[\mu\frac{\partial}{\partial\mu}+\beta(g^2)\frac{\partial}{\partial g^2}\right]\Lambda=0, \tag{B.12}$$

with Λ of the form

$$\Lambda=\mu\exp\left\{-\int^{g^2}\mathrm{d}u\,\frac{1}{\beta(u)}\right\} \tag{B.13}$$

and the (nonsingular) standard convention for fixing the integration constant is

$$\Lambda=\mu\exp\left(-\frac{1}{b_0g^2}\right)\left(b_0g^2\right)^{-b_1/b_0^2}\lambda(g^2) \tag{B.14}$$

with

$$\lambda(g^2)=\exp\left\{-\int_0^{g^2}\mathrm{d}u\left(\frac{1}{\beta(u)}+\frac{1}{b_0u^2}-\frac{b_1}{b_0^2u}\right)\right\}. \tag{B.15}$$

We combine eqs. (B.14) and (B.7) to derive

$$t=-\log(\Lambda x)=\frac{1}{b_0\bar{g}^2}+\frac{b_1}{b_0^2}\log\left(b_0\bar{g}^2\right)-\log\left(\lambda(\bar{g}^2)\right). \tag{B.16}$$

This is inverted for large s, t,

$$s=t+\frac{\log t}{n-2}\left(1+\frac{1}{(n-2)t}\right)-\frac{1}{4(n-2)t}+\mathrm{O}\left(\frac{\log^2 t}{t^2}\right). \tag{B.17}$$

With eq. (B.17) inserted in (B.11) we have found the universal perturbative short distance behavior,

$$G\propto\left\{t+\frac{1}{n-2}\left[\log t+1+(n-2)a+\frac{\log t}{(n-2)t}\right.\right.$$
$$\left.\left.+\left(a-\frac{n-3}{2(n-2)}\right)\frac{1}{t}\right]\right\}^{(n-1)/(n-2)}\left(1+\mathrm{O}\left(\frac{\log^2 t}{t^3}\right)\right). \tag{B.18}$$

Since all non-universal features of the preceding construction referred to the MS scheme, the scale Λ in $t=-\log(\Lambda x)$ is actually $\Lambda_{\overline{\mathrm{MS}}}$. It is related to the more

standard $\Lambda_{\overline{\rm MS}}$ [5] by

$$\Lambda_{\overline{\rm MS}} = 2\sqrt{\pi}\, e^{\Gamma'(1)/2}\Lambda_{\rm MS}. \tag{B.19}$$

To the order up to which we are expanding the scheme-change is implemented by the substitutions

$$t \to t' = -\log(\Lambda_{\overline{\rm MS}} x),$$

$$a \to a' = a + \tfrac{1}{2}(\Gamma'(1) + \log(4\pi)) = \Gamma'(1) + \log(2) \tag{B.20}$$

in (B.18).

We may even consider the whole family of schemes with $\Lambda_c = \exp(c)\Lambda_{\overline{\rm MS}}$ and re-expand in $t_c = -\log(\Lambda_c)$. Then the two-point function at short distance is

$$G \propto \left\{ t_c + \frac{1}{n-2}\left[\log t_c + 1 + (n-2)(a'+c) + \frac{\log t_c}{(n-2)t_c} + \left(a' + c - \frac{n-3}{2(n-2)} \right) \frac{1}{t_c} \right] \right\}^{(n-1)/(n-2)} \left(1 + O\left(\frac{\log^2 t_c}{t_c^3} \right) \right). \tag{B.21}$$

If the perturbation series could be summed, then the function on the right-hand side in (B.21) should not depend on c for fixed $\Lambda_{\overline{\rm MS}}$. This is, however, not true as we truncate the series. In fitting data with (B.21) we may treat c as a free parameter that is optimized, and we thus hope to minimize or at least develop a feeling for the effects of the remainder of the series. Similar ideas have been discussed for QCD in ref [21].

References

[1] A.M. Polyakov, Phys. Lett. B59 (1975) 79
[2] R.H. Swendsen and J.S. Wang, Phys. Rev. Lett. 58 (1987) 86
[3] U. Wolff, Phys. Rev. Lett. 62 (1989) 361
[4] U. Wolff, Nucl. Phys. B322 (1989) 759
[5] M. Lüscher, Phys. Lett. B118 (1982) 391; Nucl. Phys. B219 (1983) 233
[6] I. Bender, W. Wetzel and B. Berg, Nucl. Phys. B269 (1986) 389
[7] S.H. Shenker and J. Tobochnik, Phys. Rev. B22 (1980) 4462;
B. Berg and M. Lüscher, Nucl. Phys. B190 [FS3] (1981) 412;
G. Fox, R. Gupta, O. Martin and S. Otto, Nucl. Phys. B205 [FS5] (1982) 188;
R. Fukugita and Y. Oyanagi, Phys. Lett. B123 (1983) 71;
B. Berg, S. Meyer and I. Montvay, Nucl. Phys. B235 [FS11] (1984) 149;
A. Hasenfratz and A. Margaritis, Phys. Lett. B148 (1984) 129
[8] G. Parisi, R. Petronzio and F. Rapuano, Phys. Lett. B128 (1983) 418
[9] U. Wolff, Nucl. Phys. B300 [FS22] (1988) 501
[10] N. Madras and A.D. Sokal, J. Stat. Phys. 50 (1988) 109
[11] M. Lüscher, Cargèse Lectures (September 1983)

[12] B. Aebischer, Thesis, Bern University (November 1984)
[13] E.G. Floratos and D. Petcher, Nucl. Phys. B252 (1985) 689
[14] S. Hikami and E. Brezin, J. Phys. A11 (1978) 1141
[15] M. Falcioni and A. Treves, Phys. Lett. B159 (1985) 140; Nucl. Phys. B265 [FS15] (1986) 671
[16] U. Wolff, Nucl. Phys. B265 [FS15] (1986) 537
[17] L.F. Abott, Nucl. Phys. B185 (1981) 189
[18] M. Lüscher, Ann. Phys. (N.Y.) 142 (1982) 359
[19] M. Lüscher, private communication
[20] A. McKane and M. Stone, Nucl. Phys. B163 (1980) 169
[21] P.M. Stevenson, Phys. Rev. D16 (1981) 2916
[22] S. Samuel, O. Martin and K. Moriarty, Phys. Lett. B153 (1985) 87